

## Equilibrium Properties of a Bromine-Bromide Electrolyte for Flow Batteries

To cite this article: Mattia Duranti *et al* 2020 *J. Electrochem. Soc.* **167** 100523

View the [article online](#) for updates and enhancements.



# Equilibrium Properties of a Bromine-Bromide Electrolyte for Flow Batteries

Mattia Duranti,<sup>1,2,z</sup>  Edoardo Gino Macchi,<sup>2</sup> and Luigi Crema<sup>2</sup> 

<sup>1</sup>Department of Industrial Engineering, University of Trento, Italy

<sup>2</sup>Center for Materials and Microsystems, Fondazione Bruno Kessler, Trento, Italy

The bromine-bromide redox couple is a promising solution for aqueous cathodes of several flow batteries. In this work, we present an experimental characterization of the system  $\text{Br}_2\text{-HBr-H}_2\text{O}$  at chemical equilibrium, featuring isothermal measurements of Open Circuit Voltage (OCV), density and conductivity in solutions with concentrations up to 2 M  $\text{Br}_2$  and 4 M HBr. An equilibrium model considering polybromides formation that fits experimental data with an accuracy of 1.8 mV is presented. Information on activity coefficients and equilibrium constants of polybromides can be extrapolated from the model. Furthermore, alternative approaches are considered to effectively fit the measured voltage using algebraic equations, that provide a convenient tool for flow battery modeling at system-level.

© 2020 The Electrochemical Society ("ECS"). Published on behalf of ECS by IOP Publishing Limited. [DOI: [10.1149/1945-7111/ab98a7](https://doi.org/10.1149/1945-7111/ab98a7)]

Manuscript submitted February 7, 2020; revised manuscript received March 27, 2020. Published June 11, 2020.

Redox Flow Batteries (RFBs) are a promising technology for the storage of large amounts of energy from intermittent and irregular renewable sources today available all over the world. RFBs feature low system complexity, high round trip efficiency and potentially low costs<sup>1</sup>; the technology benefits from an easy scalability toward large sizes and can be smoothly upgraded to different capacity sizes because of the physical separation between power related components (i.e., cells and their electrode active area) and energy related components (i.e., tanks and their electrolyte capacity).<sup>2</sup>

Researchers explored several possible electrolytes for RFBs, ranging from metal ion-based ones (e.g. all-vanadium, all-iron), halogens and more recently redox active organic materials.<sup>2,3</sup> Selected chemistries, such as all-vanadium and zinc-bromide, have been scaled up to commercially available systems, while other promising chemistries are still under study.<sup>2</sup>

Flow batteries relying on bromine-based electrolytes increased in popularity as zinc-bromide RFBs entered the market and new negolytes were tested.<sup>4</sup> Specifically, research institutions and companies focused on hydrogen-bromine ( $\text{H}_2\text{-Br}_2$ )<sup>5,6</sup> and quinone-bromine (AQDS- $\text{Br}_2$ ) RFBs<sup>7,8</sup> in the last years, aiming to obtain higher energy and power densities.<sup>9</sup> Both technologies use an acidic electrolyte on the cathode side containing bromine and hydrobromic acid in aqueous solution.

Concentrations of commercially available hydrobromic acid solutions (up to 48 wt% HBr) lead to a theoretical energy density of  $200 \text{ Wh l}^{-1}$ , leaving a 2 M HBr solution as fully charged electrolyte and using a hydrogen fueled anode. High concentrations of bromine ( $\text{Br}_2$ ) and bromide ions ( $\text{Br}^-$ ) reduce both mass transport limitations and charge transfer resistance, leading to a good voltage efficiency and high power densities.<sup>10</sup> At the same time, HBr in aqueous solution leads to a very high electrolyte conductivity of around  $500 \text{ mS cm}^{-1}$ .<sup>11</sup> However, performance limitations arise during the battery design process, mainly depending on stack, membrane and electrodes structures, together with physico-chemical properties of the solutions encountered along the batteries' states of charge (SoC).

Polybromides  $\text{Br}_{2n+1}^-$  have been known for a long time to form in solutions containing bromine and bromide.<sup>12,13</sup> Several attempts were made in the last century to measure their equilibrium constants at low bromine concentrations.<sup>14,15</sup> However, there is no study available for highly concentrated electrolytes, such as the ones used in RFBs (e.g.  $C_{\text{Br}_2} > 1 \text{ mol l}^{-1}$ ). In particular, there is no established method to evaluate the electrochemical activity of bromine, bromide ions and polybromides in highly concentrated solutions, or their actual concentrations.

In this work we explore the equilibrium properties of the three-component system  $\text{Br}_2\text{-HBr-H}_2\text{O}$  over a wide range of concentrations, up to 2 M  $\text{Br}_2$  and 4 M HBr. The study aims to investigate the range of electrolyte compositions encountered during battery design and gather experimental data on physico-chemical properties of the different solutions.

Open circuit voltage (OCV), volumes of different phases and conductivity have been measured on the same solutions using direct or indirect techniques. This analysis aims at characterizing the electrolyte independently of the choice of starting compositions, range for charge-discharge cycles and possible changes of concentrations due to osmotic balancing. Therefore, the study is meant to be a reference for the analysis of a bromine-bromide half cell when poisoning and contamination can be excluded.

The work also includes two alternative approaches to represent the measured OCV data: A) a chemical equilibrium model that aims to obtain quantitative information on equilibrium constants for polybromides formation and on the activity of all species in solution; B) a single equation model aiming to represent the measured data. Following on, the manuscript is organized in four sections: 2) describes experimental methods, 3.1) explains models architecture and fitting techniques, 3.2) shows experimental results and gives a comparison with the discussed modeling, and 4) summarizes the achievements and concludes.

## Experimental

The Open Circuit Voltage was measured in a jacketed three electrodes setup (Gamry Eurocell) using a Biologic SP-150 potentiostat and following a potentiometric Stepwise Titration (ST) procedure. Automatic titration was considered inappropriate because of the high volatility and highly corrosive behavior of bromine: commercially available titrators can be strongly damaged by such aggressive chemicals. A comparison between manual Stepwise Titration (ST) and Continuous Titration (CT) was performed, as shown in Fig. 1. Potentiometric ST consists in recording the OCV vs a reference, while adding progressively finite volumes of a liquid (bromine) to a solution with a specified starting concentration. After electrochemical equilibrium in the resulting solution is achieved (assumed here as  $dV/dt < 10^{-3} \text{ mV s}^{-1}$ ), an OCV value is recorded and another titrant volume is added. In potentiometric CT instead, a burette drops bromine continuously and the OCV is recorded, while the dropped volume is simultaneously recorded. Potentiometric tests on a solution with addition of complexing agent (4 M HBr 0.7 M MEP) showed that CT can overestimate the OCV value of about 10 mV at very high concentrations<sup>16</sup> (Fig. 1). We therefore used potentiometric ST, because it was considered safer in handling bromine and more accurate than manual CT.

<sup>z</sup>E-mail: [mattia.duranti@unitn.it](mailto:mattia.duranti@unitn.it)

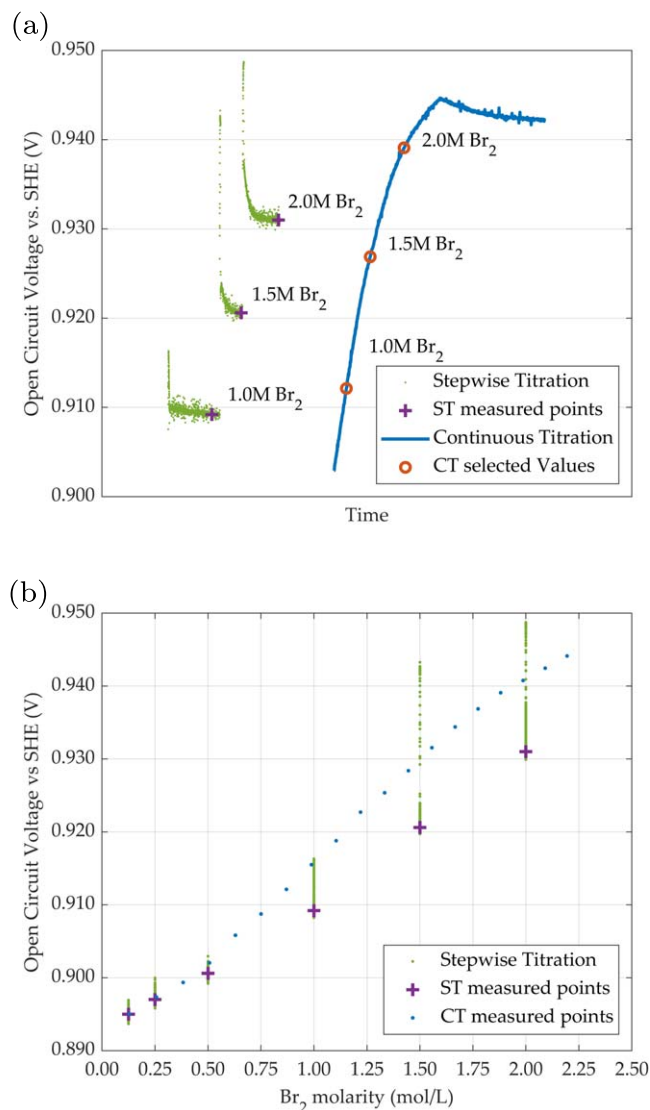


**Figure 1.** Comparison between potentiometric stepwise titration (ST) and continuous titration (CT) processes (a) over time and (b) over total bromine concentration on a 4 M HBr 0.7 M MEP solution. Green dots show potentiometric ST; blue line show potentiometric CT; violet crosses show ST measured points; blue dots show CT measured points; red circles show the selected values in CT corresponding with ST measured points at round molarities; with permission.<sup>16</sup>

Pure bromine was titrated in consecutive finite volumes into seven water-hydrogen bromide solutions having different concentrations in the range 0.125 M–4 M HBr, and obtaining data-points in the range 0 M–2 M Br<sub>2</sub>. Starting solutions were prepared by mixing deionized water and reagent grade 48 wt% hydrobromic acid from Sigma Aldrich. Finite volumes of bromine were prepared in order to obtain round molarities after the addition. The molarity of HBr is not constant through the titration process, therefore either molarity of the starting solution  $C_0$  or molality  $m$  is indicated for HBr in the graphs below. Total concentration values shown in this work were calculated using the density measurements explained below. The uncertainty on these concentrations was evaluated considering both the uncertainty of density and the precision of the equipment used for preparing each solution, resulting in a maximum value of  $2 \cdot 10^{-4} \text{ mol l}^{-1}$  for all concentrations below 1 M and  $0.01 \text{ mol l}^{-1}$  for all other concentrations.

The voltage was recorded vs an Ag/AgCl/sat.KCl reference electrode, a platinum ring acted as working electrode and a graphite rod was used as counter electrode. The cell was kept at 25.0 °C by a

steady water flow in the jacket. The setup was previously tested with Fe<sup>(II)</sup>/Fe<sup>(III)</sup> redox couple in 4 M HCl electrolyte, achieving an OCV accuracy of 3 mV. A value of 0.197 V was added to the measured voltages to obtain values vs standard hydrogen electrode (SHE). To avoid possible poisoning from bromine or bromide ions, the Ag/AgCl electrode was periodically tested vs an HgSO<sub>4</sub> reference electrode, connecting them by a saturated KCl salt bridge, and eventually refreshed. The whole ST procedure was repeated multiple times, showing an average deviation within the stated accuracy.

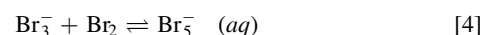
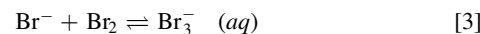
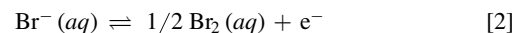
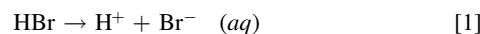
Electrical conductivities were indirectly obtained by performing electrochemical impedance spectroscopy after each OCV acquisition. To obtain a relative resistivity, the measured impedance value was divided by the impedance value of the starting solution from the same setup. Impedance values were selected at the highest frequency that showed purely ohmic behavior and averaged between two different measurements.

Volumes were evaluated by a ST procedure in graduated phials, which guaranteed an accuracy of 0.1 ml on total volumes of 8 ml at different HBr concentrations. After the addition of each bromine drop, the phials have been centrifuged at 1000 rpm for 1 min to gather possible liquid particles stuck to lids and glass walls. For every data-point, we registered the total volume and the amount of undissolved liquid bromine.

## Results and Discussion

**Modeling.**—In this section, we provide two alternative approaches to fit the measured OCV data: A) a model considering formation of polybromides and resolution of side reactions equilibrium; B) a single equation model reducing the electrolyte behavior to activity coefficients for the total amount of bromine and hydrobromic acid in the electrolyte. The first approach is a faithful interpretation of the physico-chemical processes involved in the development of electrochemical equilibrium, while the second is an empirical representation of the measured data, which can be a useful tool for more complex models featuring a bromine-bromide electrolyte, such as dynamic simulation of battery systems. Interpretations and considerations following from the two presented approaches are discussed in the results section.

**Equilibrium model (A):** In this physico-chemical electrolyte model, we consider the following reactions:



Hydrobromic acid is considered fully dissociated along this work, due to its very low pKa. Solubility of bromine in water is reported to be  $0.2141 \text{ mol l}^{-1}$ .<sup>17</sup> While data on bromine solubility in HBr solutions are not available, scientific literature reports bromine solubility in NaBr solutions of  $1.24 \text{ mol l}^{-1}$  in 1 M NaBr, strongly increasing with salt concentration.<sup>17</sup> Equilibrium constant for bromine induced hydrolysis is widely reported to be less than  $10^{-8}$  in neutral solutions and it diminishes with acidity.<sup>15</sup> Therefore, the occurrence of such phenomenon has been neglected.

Equation 6 defines two equilibrium constants of tribromide and pentabromide formation.

$$K_3 = \frac{\gamma_3}{\gamma_1 \gamma_a} \frac{[\text{Br}_3^-]}{[\text{Br}^-][\text{Br}_2]}, \quad K_5 = \frac{\gamma_5}{\gamma_3 \gamma_a} \frac{[\text{Br}_5^-]}{[\text{Br}_3^-][\text{Br}_2]} \quad [6]$$

In the following, we are forced to assume that activity coefficients of all the polybromides are equal to each other and to the one of

bromide ion:  $\gamma_{\pm} = \gamma_5 = \gamma_3 = \gamma_1$ , since they are impossible measure separately. This hypothesis is coherent with the theoretical notion that cations (i.e.,  $H^+$ ) and anions (i.e.,  $Br^-$ ,  $Br_3^-$ ,  $Br_5^-$ ) in the same electrolyte share the same mean activity coefficient. The activity coefficient of bromine  $\gamma_a$  is expected to follow the salting-out behavior of apolar dissolved gases (Setschenow equation). The activity coefficients are expressed by Eqs. 7 and 8,

$$\gamma_a = c_1 I, \quad [7]$$

$$\gamma_{\pm} = -\frac{A\sqrt{I}}{1 + aB\sqrt{I}} + bI + cI^2, \quad [8]$$

where  $A = 0.510 \ell^{0.5} \text{mol}^{-0.5}$  and  $B = 3.288 \ell^{0.5} \text{mol}^{-0.5} \text{nm}^{-1}$  are Debye-Hückel coefficients for aqueous solutions,  $I = [HBr]_{tot}$  is the ionic strength, and  $\hat{a}$ ,  $b$ ,  $c$ ,  $c_1$  are fitting parameters. Elaboration of data reported by Jones et al.<sup>14</sup> on activity of bromine in potassium nitrate solutions leads to  $c_1 = 0.0577 \ell/\text{mol}$ . Fitting the isopiestic measurements from Macaskill et al.<sup>18</sup> of activity coefficients of pure hydrobromic acid solutions leads to  $\hat{a} = 0.4863 \text{ nm}$ ,  $b = 0.1356 \ell/\text{mol}$  and  $c = 0.0093 \ell^2/\text{mol}^2$ . Molar balances of bromine and bromide ion are written respectively as

$$[Br_2]_{tot} = [Br_2] + [Br_3^-] + 2[Br_5^-] \quad [9]$$

$$[HBr]_{tot} = [Br^-] + [Br_3^-] + [Br_5^-]. \quad [10]$$

In this representation, only aqueous free bromine and bromide ions (i.e., not bounded in a polybromide chain) are considered electrochemically active. Thus, Nernst equation is written as

$$OCV = E_{Br^-, Br_2}^{\circ} - \frac{RT}{F} \log \frac{\gamma_{\pm}[Br^-]}{\gamma_a^{1/2}[Br_2]^{1/2}}, \quad [11]$$

where  $E_{Br^-, Br_2}^{\circ} = 1.0873 \text{ V}$  is the standard redox potential of Reaction 2. Polybromides are not considered to take part in the redox reaction. Nonetheless, they affect the equilibrium voltage by

defining the amount of bromine and bromide ions left free in the aqueous phase.

Starting from the known total concentrations of  $Br_2$  and  $HBr$ , 6, 9 and 10 constitute a non-linear system of four equations, which can be numerically solved for different values of the parameters  $K_3$ ,  $K_5$  and thus, fitted to experimental OCV data using Eq. 11. The fit was performed using a Levenberg-Marquardt algorithm for non-linear problems.

*Single equation empirical model (B):* In the single equation electrolyte model, we only consider reactions 1, 2 and 5. The activity of the  $Br^-$  is considered equal to the mean activity of  $HBr$ , following  $a_{Br^-} = \hat{\gamma}_{\pm} [HBr]_{tot}$ , while the behavior of  $Br_2$  is modeled as  $a_{Br_2} = \hat{\gamma}_a [Br_2]_{tot}$ . Both activity coefficients used in this approach may depend on the ionic strength  $I = [HBr]_{tot}$  and on the total concentration of bromine in aqueous phase  $[Br_2]_{tot}$ . For every OCV data-point, the activity coefficients can be grouped in a single parameter  $\psi = \hat{\gamma}_{\pm} \hat{\gamma}_a^{-1/2}$ , which can be evaluated by an inverse Nernst equation in the form

$$\psi = \frac{[Br_2]_{tot}^{1/2}}{[HBr]_{tot}} \exp\left(\frac{F(E_{Br^-, Br_2}^{\circ} - OCV)}{RT}\right). \quad [12]$$

In this modeling framework,  $\psi$  aggregates all deviations from ideal electrolyte behavior, including formation of polybromides, possible presence of undissociated acid and deviation of the activity of all redox active components from ideality. Several models were used to evaluate  $\hat{\gamma}_{\pm}$  and  $\hat{\gamma}_a$  in order to find a best fit of the available data. A list of the equations considered in this process is presented in Table I, including B-dot equation, Standard Interaction Theory (SIT) equations<sup>19</sup> and others for ionic species,<sup>20</sup> Setschenow equation<sup>21</sup> and SIT equations for uncharged species.<sup>22</sup>

#### Experimental results and fitting.—Volume and conductivity:

Figs. 2a and 2b show the results from volume measurements. At low  $HBr$  concentrations and relatively high  $Br_2$  concentrations a second bromine-rich liquid phase appeared. The increase in volume of the non-aqueous liquid phase follows a linear behavior, in agreement

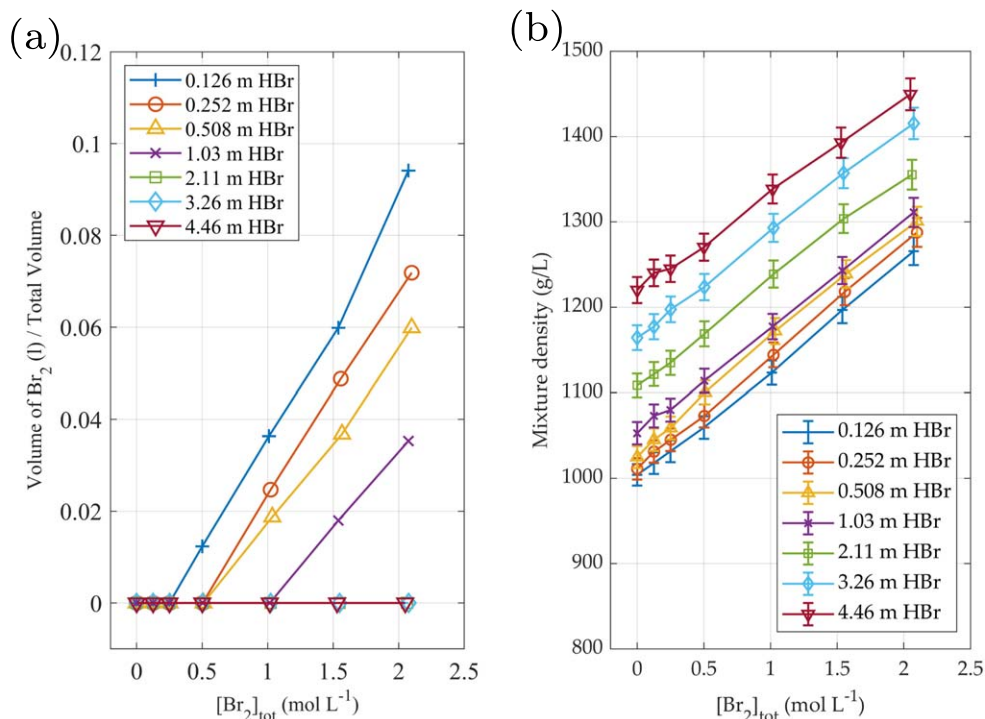


**Figure 2.** (a) volume of undissolved liquid bromine over total volume of the mixture and (b) density of the mixtures for different solutions of  $HBr$  from  $0.126 \text{ mol kg}^{-1}$  to  $4.46 \text{ mol kg}^{-1}$ ; measured points are represented by symbols, while lines between symbols highlight the trends; different symbols and colors corresponds to different  $HBr$  solutions; estimated uncertainty of the mixture density is represented by vertical error bars.

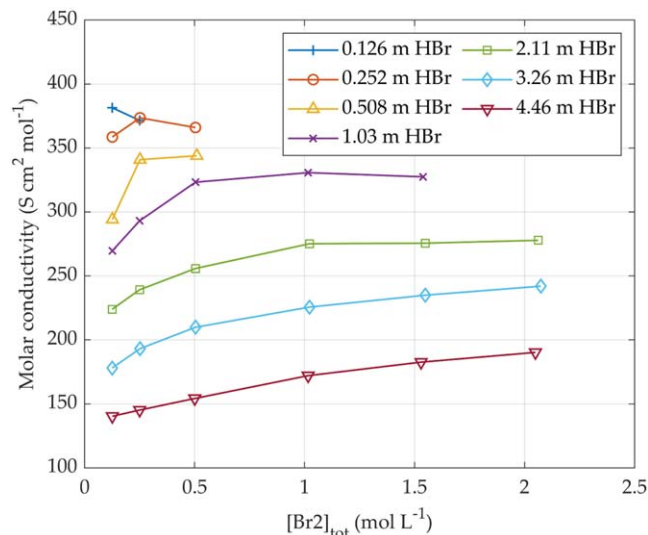


**Figure 3.** Molar conductivity from EIS performed in the aqueous phase vs  $\text{Br}_2$  concentration; shown values are obtained by dividing the measured conductivity by HBr molarity; experimental results are expressed by mark connected with lines to highlight the trends.

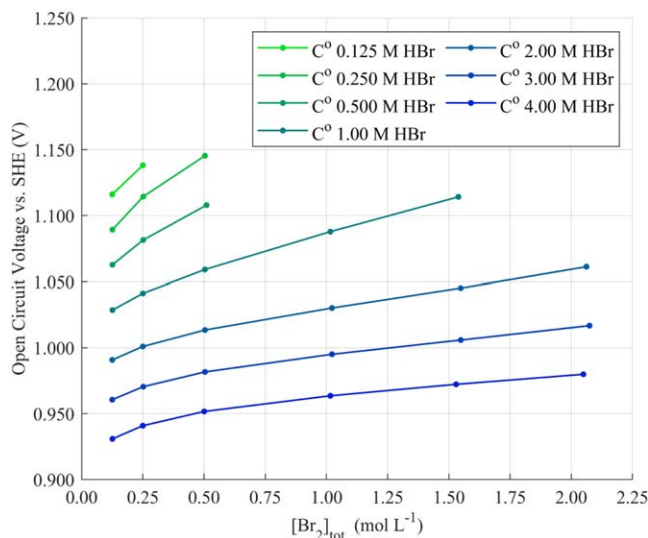


**Figure 4.** Results of OCV measurements using potentiometric ST procedure; points of different colors correspond to titration tests performed with different starting solutions of HBr, featuring concentration  $C^\circ$ ; lines connecting measured points highlight the trends; data-points showing two phases are not shown.

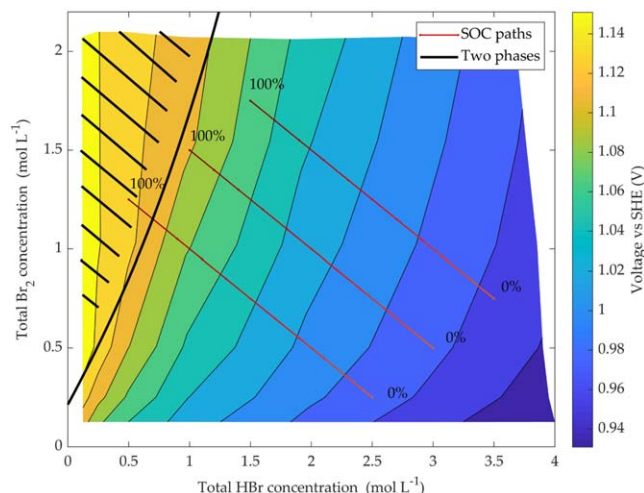


**Figure 5.** Representation of experimental results from OCV measurements and possible battery SOC paths; the color map shows the open circuit voltage interpolated between measured values; red lines shows possible SoC paths for different choices of starting compositions and a charge-discharge range of  $1 \text{ mol l}^{-1}$  of  $\text{Br}_2$ ; the region confined by black lines shows the experimental appearance of two phases.

with the accumulation of pure bromine. Density was calculated for each data point from volume measurements and known masses. When the electrolyte split into two phases, total volume and density were evaluated considering both phases.  $[\text{HBr}]_{\text{tot}}$  and  $[\text{Br}_2]_{\text{tot}}$  were then calculated using these density values.

Results of conductivity measurements are shown in Fig. 3.

The molar conductivity of each data-point was obtained using literature values of absolute conductivity in HBr solutions<sup>11</sup> through the formula

$$\Lambda = \frac{\kappa^\circ \hat{R}^\circ}{\hat{R}} \frac{1}{[\text{HBr}]_{\text{tot}}}, \quad [13]$$

where  $\hat{R}$  is the measured resistance of a specific data-point,  $\hat{R}^\circ$  is the measured resistance of the starting solution,  $\kappa^\circ$  is the conductivity from literature of the HBr solution with concentration equal to the starting solution and  $[\text{HBr}]_{\text{tot}}$  is the actual concentration of HBr of the considered data-point. In general, molar conductivity shows a slight increase with bromine at moderate bromine concentrations, stabilizing at higher concentrations.

*Open circuit voltage analysis:* Results of the OCV measured by potentiometric ST are shown in Figs. 4 and 5.

Samples with a total concentration resulting in the deposition of a second liquid phase showed a constant OCV with further addition of

**Table I.** List of equations adopted to fit OCV data using the single equation empirical model (Model B).

Abbr.	Model Name	$\log_{10} \hat{\gamma}_{\pm}$	$\log_{10} \hat{a}$	Fitted parameters
B1	B-dot	$-\frac{A\sqrt{I}}{1+\hat{a}B\sqrt{I}} + bI$	0	$\hat{a}, b$
Bm	Bromley	$-\frac{A\sqrt{I}}{1+\hat{a}B\sqrt{I}} + \frac{0.06+0.6b}{1+1.5I} + bI$	0	$\hat{a}, b$
Q	Quadratic	$-\frac{A\sqrt{I}}{1+\hat{a}B\sqrt{I}} + bI + cI^2$	0	$\hat{a}, b, c$
B2	B-dot/Salting-out	$-\frac{A\sqrt{I}}{1+\hat{a}B\sqrt{I}} + bI$	$c_1 I$	$\hat{a}, b, c_1$
B3	B-dot/SIT	$-\frac{A\sqrt{I}}{1+\hat{a}B\sqrt{I}} + bI$	$c_1 I + c_2 [\text{Br}_2]_{\text{tot}}$	$\hat{a}, b, c_1, c_2$
SIT1	SIT	$-\frac{A\sqrt{I}}{1+\hat{a}B\sqrt{I}} + bI + b_2 [\text{Br}_2]_{\text{tot}}$	0	$\hat{a}, b, b_2$
SIT2	SIT/Salting-out	$-\frac{A\sqrt{I}}{1+\hat{a}B\sqrt{I}} + bI + b_2 [\text{Br}_2]_{\text{tot}}$	$c_1 I$	$\hat{a}, b, b_2, c_1$
SIT3	SIT/SIT	$-\frac{A\sqrt{I}}{1+\hat{a}B\sqrt{I}} + bI + b_2 [\text{Br}_2]_{\text{tot}}$	$c_1 I + c_2 [\text{Br}_2]_{\text{tot}}$	$\hat{a}, b, b_2, c_1, c_2$

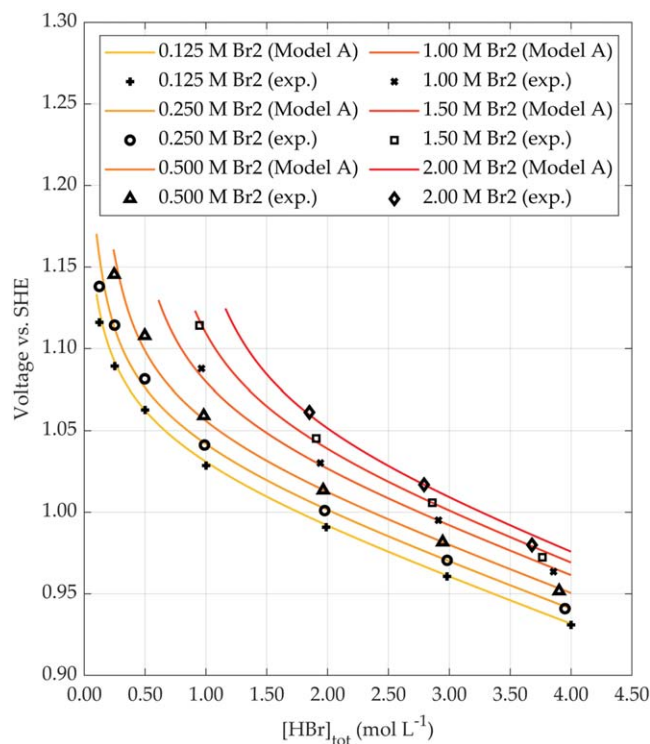


**Figure 6.** Fitting lines of the equilibrium model (Model A) and experimental OCV data; black symbols with different shapes represent measured OCV values at different  $\text{Br}_2$  molarity; colored lines show the model results at different  $\text{Br}_2$  molarities.

pure bromine. Volume and conductivity of the aqueous phase measured in such solutions also did not show variations when more bromine was added, suggesting that pure insoluble bromine was accumulating in a separate liquid phase. Therefore, the corresponding data-points were excluded from the OCV analysis, assuming they were repetitions of the same aqueous phase data.

OCV data show values sensibly lower than those deduced using the classic Nernst equation, especially at high HBr concentrations. This highlights the need for developing a more realistic equilibrium model. A fit of the experimental OCV data with the equilibrium

model (Model A) presented above was performed. Values of both experimental and fitted OCV are shown in Fig. 6.

Given the strongly non-linear behavior of the system, a preliminary analysis was performed to assess the impact of each parameter on the solution and to define suitable fitting ranges. This investigation showed that our OCV data could not be properly fitted using Macaskill's activity coefficient for pure HBr solutions.<sup>18</sup> This could be expected since polybromides, that do not form in pure HBr solutions, are here present. In fact, the parameter used in our model is a mean activity coefficient of hydrogen, bromide, tribromide and pentabromide ions together, while Macaskill's coefficient averages the first two only. Moreover, we noticed that  $c_1$  has very little impact due to the small amount of free bromine in the aqueous phase. Thus, we proceeded by fitting  $K_3$ ,  $K_5$ ,  $\hat{a}$ ,  $b$  and  $c$  until convergence, obtaining a  $R^2$  value of 0.9992 and a root mean square error on the measured OCV of 1.79 mV. Values of fitted parameters are listed in Table II.

Predictions on the concentration of free bromine, bromide, tribromide and pentabromide ions in the aqueous phase from Model A using parameters from Table II are shown in Figs. 7a and 7b. Both figures show that polybromides formation reduces the concentration of free bromine by one or two orders of magnitude whenever excess of bromide is granted. In particular, the pentabromide ion is shown to be present in significant amount. This can explain the discrepancies between measured OCV values and values expected from classic Nernst equation, especially at high HBr concentrations.

The fitted value of  $K_5$  is higher than those reported in potassium bromide at low concentrations. However, values reported by Jones<sup>14</sup> strongly increased with concentration. Indeed, by means of a fitting analysis, it is not possible to distinguish between presence of pentabromine, eptabromide or higher polybromides, because they all affect the concentration of free bromine in the same way, subsequently lowering the OCV value by the same amount. For the sake of consistency, the parameter  $K_5$  used in this work should be considered as the sum of the equilibrium constant of formation of all the polybromides  $\text{Br}_{2n+1}^-$  with  $n \geq 2$ .

The minimum concentration of HBr able to absorb 1 mol  $\ell^{-1}$  of  $\text{Br}_2$  seems slightly smaller than that of NaBr from literature<sup>17</sup> (0.78 mol  $\ell^{-1}$ ), confirming hydrobromic acid as a very good carrier for aqueous bromine. Concentrations of aqueous free bromine shown in this model are consistent with solubility of bromine in water within the whole data-set. Figure 7a shows that aqueous free bromine reaches a concentration value similar to the solubility limit

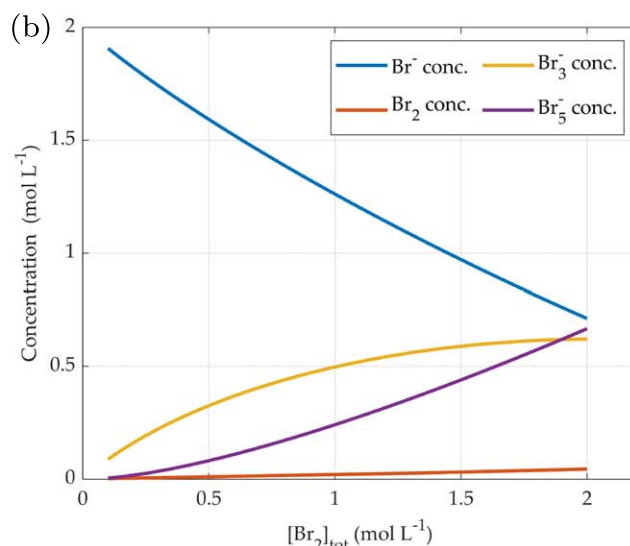
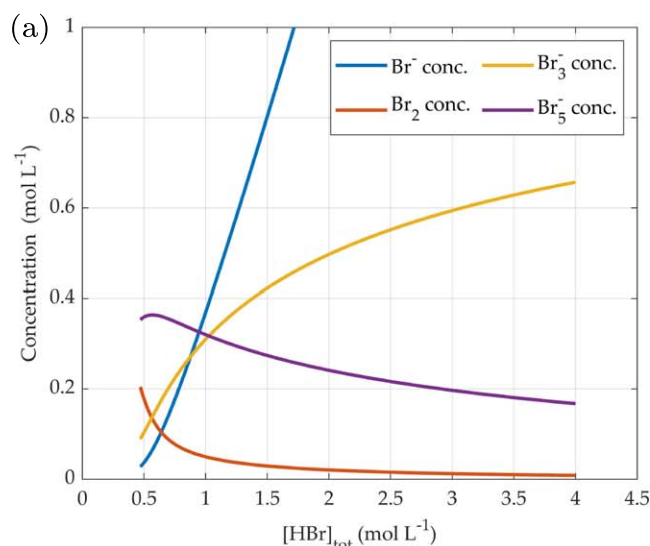


**Figure 7.** Concentration of free bromine and polybromide ions in solution ( $\text{Br}^-$ ,  $\text{Br}_2$ ,  $\text{Br}_3^-$ , and  $\text{Br}_5^-$ ) predicted with Model A using (a) constant bromine concentration of 1 M  $\text{Br}_2$ ; (b) constant bromide concentration of 2 M HBr.

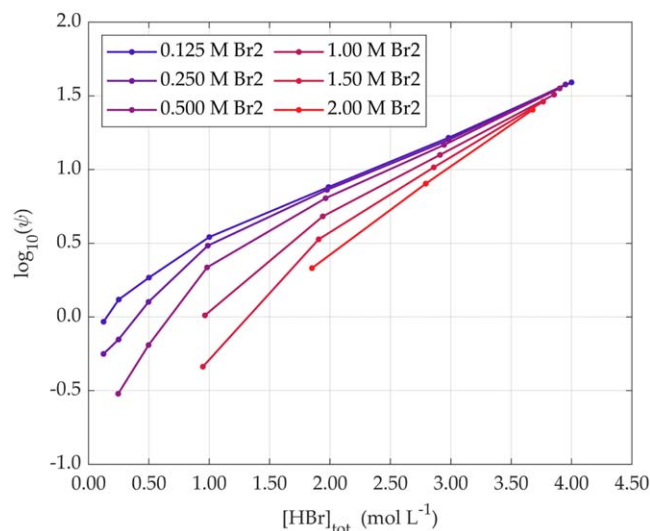


**Figure 8.** Logarithm of the parameter  $\psi$  expressed in Eq. 12 calculated from the experimental OCV data for different concentration of  $\text{Br}_2$ ; lines connect the computed points to highlight trends.

**Table II. Parameters' values obtained from the fitting of the equilibrium model (Model A).**

Parameter	Value	Unit
$\tilde{a}$	0.2022	nm
$b$	0.2281	$\ell/\text{mol}$
$c$	0.0151	$\ell^2/\text{mol}^2$
$c_1$	0.0577 <sup>a)</sup>	$\ell/\text{mol}$
$K_3$	14.18	1
$K_5$	18.51	1

a) From literature.<sup>14</sup>

of bromine in water (0.2141 M  $\text{Br}_2$ ) in an HBr solution of approximately  $0.50 \text{ mol } \ell^{-1}$ . At this very same concentration, the second liquid phase appears experimentally. This fact suggests that the formation of polybromides in aqueous phase could be the only reason for the high solubility of bromine in hydrobromic acid.

**Models comparison:** The fitting of Model A is significantly more accurate than any single equation model, which have no claim to be physically meaningful. However, a single equation representation can be very useful when more complex simulations are built on equilibrium data. Several versions of Model B based on different equations for  $\gamma_{\pm}$  were fitted to OCV data in order to find the best compromise between simplicity and accuracy. Goodness of fit for these models are shown in Table III. For the best performing ones

**Table III. Number of fitted parameters,  $R^2$ , and root mean square error (rmse) resulting from the OCV fitting performed with the single equation approach (Model B).**

Model	n. of parameters	$R^2$	rmse (mV)
B1	2	0.965	11.8
Bm	2	0.943	15.0
Q	3	0.965	11.9
B2	3	0.964	12.0
B3	4	0.978	9.64
SIT1	3	0.978	9.47
SIT2	4	0.978	9.64
SIT3	5	0.978	9.83

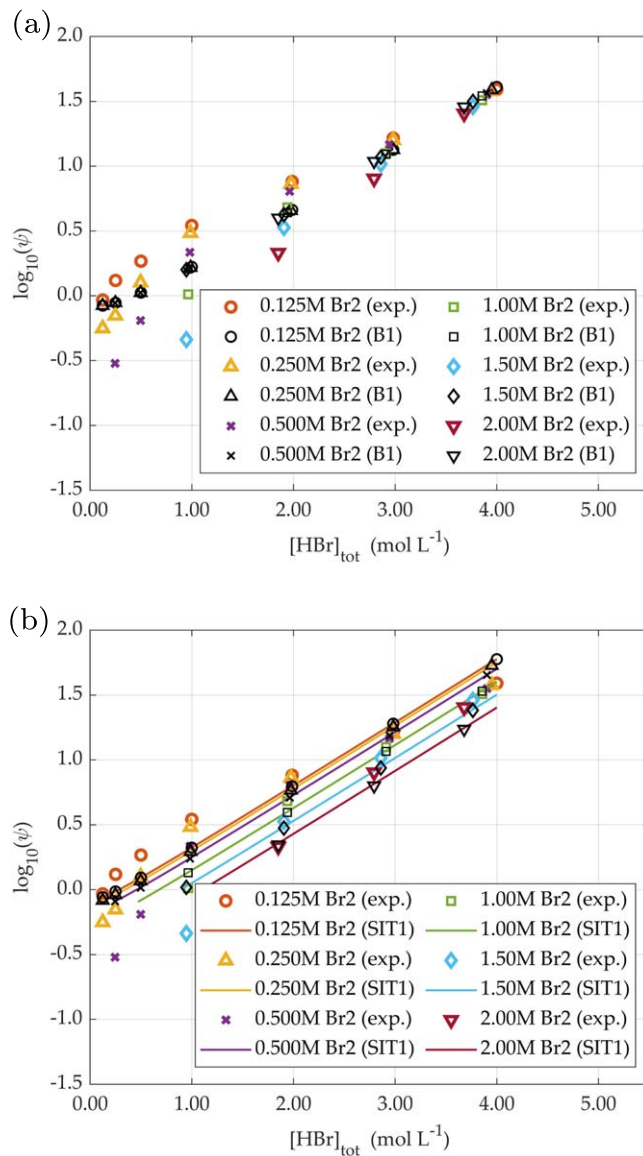


**Figure 9.** Logarithm of the parameter  $\psi$  and comparison with values obtained by fitting with single equation models (Model B); (a) fitting with model B1; (b) fitting with model SIT1; values calculated from experimental OCV are represented by colored marks; values obtained by fitting are represented by black marks; different shapes represent different bromine concentrations; the continuous lines represent simulated values from Model SIT1 at different bromine concentrations.

(B-dot, SIT) we introduced alternatives for  $\gamma_a$ , though additional parameters often did not improve fitting results.

A sharp difference in goodness of fit can be seen between i) the models that depend on ionic strength only and ii) the models which depends on both ionic strength and bromine concentration. The latter give better results reducing the root mean square errors from 12 mV to 9 mV. Experimental values of  $\psi$  accordingly shows to be function of both concentrations (Fig. 8). However, high amount of HBr increases the in-dependency of  $\psi$  from the total concentration of  $\text{Br}_2$ . This makes it possible to model OCV by one equation depending exclusively on ionic strength (such as B-dot equation) only at high HBr concentrations. This is particularly clear in Figs. 9a and 9b, which show modeled  $\psi$  for Model B1 and Model SIT1. For practical reasons, Table IV shows only results for Model B1 and Model SIT1, which are the best fitting of model type i) and ii), respectively.

Figures 10b and 10c show how model SIT1 gives a better overall representation, never excessively deviating from experimental OCV

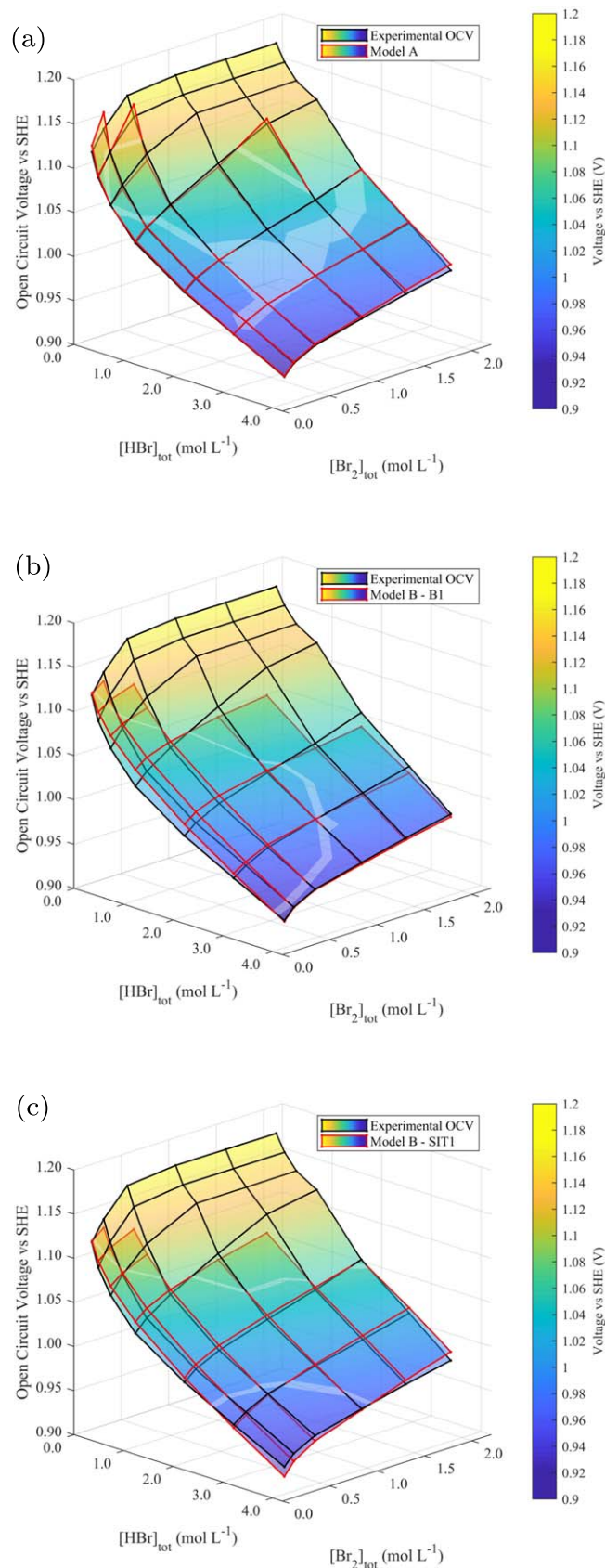


**Figure 10.** Set of 3D plots comparing fitting of different models (red edges) on OCV data (black edges): (a) shows the fitting surface using Model A, (b) using Model B1, and (c) using Model SIT1; black lines connect experimental OCV data-points and red lines connect simulated OCV values; the surfaces color scales with values on z axis.

**Table IV.** Parameters values obtained from the fitting with single equation model (Model B) for the models B1 and SIT1.

Parameter	B1	SIT1	Unit
$\hat{a}$	0.264	0.779	nm
$b$	0.496	0.492	$\ell/\text{mol}$
$b_2$	...	-0.199	$\ell/\text{mol}$

values, while model B1 results in a more accurate fit whenever high ionic strengths are involved ( $I > 2 \text{ mol } \ell^{-1}$ ).

## Conclusions

The electrochemical equilibrium properties of the  $\text{Br}_2\text{-HBr-H}_2\text{O}$  system have been experimentally investigated over a wide concentration range, namely 0.125 M–4 M HBr, 0 M–2 M  $\text{Br}_2$ . Density, electrical conductivity and equilibrium voltage of the electrolyte have been measured. A stepwise titration procedure has been adopted for the measurements. The solubility of bromine in HBr resulted to be similar to the one in NaBr, but with higher solubility limits.

A model of chemical equilibrium in the electrolyte featuring formation of polybromides has been proposed and model results have been fitted to the measured open circuit voltage data, achieving a root mean square error of 1.8 mV. Parameters for average activity coefficients of polybromides in HBr solutions and average values for constants of polybromides formation at high concentrations were extrapolated for the first time. Lastly, several single equation models for the representation of OCV data were fitted and compared, enabling to easily exploit the findings of this study in more complex simulation models.

## Acknowledgments

This work has been supported partially by direct funding of Fondazione Bruno Kessler and partially by Green Energy Storage, within the project GREENERSYS, which is funded by the Autonomous Province of Trento. The authors are grateful for the economic support received. We thank Matteo Testi, Micheal Küttinger, Ilaria Pucher and Martina Trini for the fruitful discussions.

## ORCID

Mattia Duranti <https://orcid.org/0000-0003-2345-6177>

Luigi Crema <https://orcid.org/0000-0003-3263-1766>

## References

1. A. Z. Weber, M. M. Mench, J. P. Meyers, P. N. Ross, J. T. Gostick, and Q. Liu, *Journal of Applied Electrochemistry*, **41**, 1137 (2011).
2. J. Noack, N. Roznyatovskaya, T. Herr, and P. Fischer, *Angewandte Chemie—International Edition*, **54**, 9776 (2015).
3. K. Wedege, E. Dražević, D. Konya, and A. Bienten, *Sci. Rep.*, **6**, 1 (2016).
4. M. Skyllas-Kazacos, M. H. Chakrabarti, S. A. Hajimolana, F. S. Mjalli, and M. Saleem, *J. Electrochem. Soc.*, **158**, R55 (2011).
5. V. Battaglia, A. Z. Weber, S. Haussener, P. Ridgway, K. T. Cho, and V. Srinivasan, *J. Electrochem. Soc.*, **159**, A1806 (2012).
6. G. Lin, P. Chong, V. Yarlagadda, T. Nguyen, R. J. Wycisk, P. N. Pintauro, M. Bates, S. Mukerjee, M. C. Tucker, and A. Z. Weber, *J. Electrochem. Soc.*, **163**, A5049 (2016).
7. B. Huskinson, M. P. Marshak, C. Suh, S. Er, M. R. Gerhardt, C. J. Galvin, X. Chen, A. Aspuru-Guzik, R. G. Gordon, and M. J. Aziz, *Nature*, **505**, 195 (2014).
8. Q. Chen, L. Eisenach, and M. J. Aziz, *J. Electrochem. Soc.*, **163**, A5057 (2016).
9. M. L. Perry and A. Z. Weber, *J. Electrochem. Soc.*, **163**, A5064 (2016).
10. B. Huskinson and M. J. Aziz, *Energy Science and Technology*, **5**, 1 (2013).
11. E. Care, *J. Am. Chem. Soc.*, **131**, 12862 (2009).
12. G. N. Lewis and H. Storch, *J. Am. Chem. Soc.*, **39**, 2544 (1917).



13. M. Sherrill and E. Izard, *J. Am. Chem. Soc.*, **50**, 1665 (1928).
14. G. Jones and S. Baeckström, *J. Am. Chem. Soc.*, **56**, 1517 (1934).
15. C. M. Kelley and H. V. Tartar, *J. Am. Chem. Soc.*, **78**, 5752 (1956).
16. M. Duranti, M. Testi, E. G. Macchi, and L. Crema, *IFBF Conference Book of Papers* (Swanbarton Limited, Malmesbury, UK) 1, p. 38 (2019).
17. J. M. Bell and M. L. Buckley, *J. Am. Chem. Soc.*, **34**, 14 (1912).
18. J. B. Macaskill and R. G. Bates, *Journal of Solution Chemistry*, **12**, 607 (1983).
19. P. Sipos, *Journal of Molecular Liquids*, **143**, 13 (2008).
20. D. Rowland and P. M. May, *Journal of Chemical and Engineering Data*, **60**, 2090 (2015).
21. M. Randall and C. F. Failey, *Chem. Rev.*, **4**, 285 (1927).
22. M. P. Elizalde and J. L. Aparicio, *Talanta*, **42**, 395 (1995).